Fractional-Order Models for Platooning Systems: The Relationship between Order and PD Gains through Hybrid Optimization

Jiajun Cui[1] and Bill Goodwine[2]

***Abstract*— This paper investigates the performance of a reduced-order fractional dynamic model for representing a large platooning system, with a focus on the relationship between the order of a fractional model and control gains used in the platooning system. For the large platooning system we modeled, each vehicle in the system applies an identical proportional-derivative (PD) controller and only responds to the immediately preceding vehicle. We employ an optimization-based method to find the best-matched model parameters under different PD control gains. Specifically, to avoid artifacts from the optimization process, we apply a hybrid particle swarm and pattern search method to optimize the model parameters. For comparison, we use a second-order differential equation model as a benchmark against our fractional-order model. The results show an intuitive relationship between the model's fractional order and the control gains. Specifically, increasing the proportional gain kp leads to a higher fractional order, and increasing the derivative gain kd results in a lower fractional order. Moreover, the fractional reduced-order model outperforms the integer reduced-order model when the optimal fractional order lies between 1 and 2, especially in the middle. These results have the potential to lead us to find a better reduced-order model for platooning systems and provide more insight into solving difficult control problems such as string stability.**

I. Introduction

Fractional order differential equations (FODEs) have attracted increasing interest recently. FODEs are a generalization of integer-order differential equations, where the order is non-integer. Some textbooks about fractional calculus include [1]–[3]. Compared to integer-order derivatives that use only local information of the function near a point, fractional-order derivatives are global and use all previous values of the function.

Due to the non-local nature of the fractional derivative, FODEs are often more promising in modeling system dynamics with infinite states or memories [4]. FODEs can be applied in many fields. For example, many complex, large-scale systems may exhibit fractional order dynamics since the internal components within such systems often have complicated interactions with each other [5], [6]. These complicated interactions may lead to non-local dynamics. FODEs are used to model analog electronic circuits [7], viscoelastic material behaviors [8], [9], and large complex systems [10].

[1]Jiajun Cui is with the Department of Aerospace and Mechanical Engineering, University of Notre Dame, Notre Dame, Indiana 46556 USA jcui3@nd.edu

[2]Bill Goodwine is with the Department of Aerospace and Mechanical Engineering, University of Notre Dame, Notre Dame, Indiana 46556 USA bill@controls.ame.nd.edu.

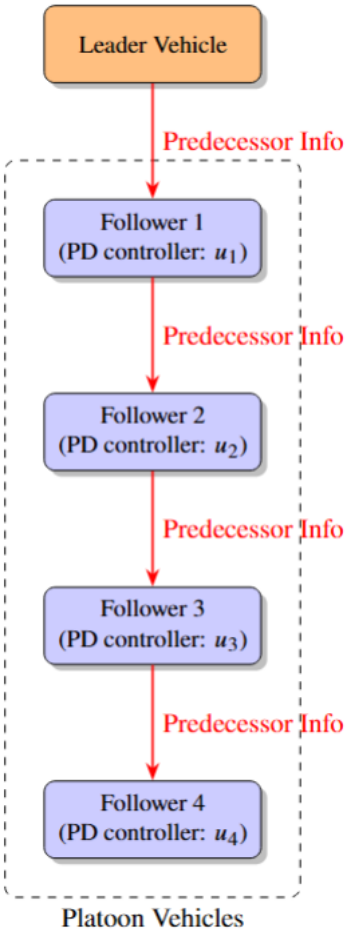

Fig. 1. Platoon system with a proportional-derivative (PD) control and only responding to the immediately preceding vehicle.

For systems that present significant fractional order dynamics, a control algorithm needs to be designed to address the fractional order nature of the system [11]. Another way to utilize fractional dynamics is fractional order controllers, such as the fractional PID controller [12] and the CRONE controller [13]. The fractional derivative in the controller allows the researchers to have more degrees of freedom in the controller design, which leads to better performance and robustness of the control system [14], [15].

Vehicle platooning control is a promising approach to improve traffic efficiency and thus has attracted much attention. A vehicle platooning system is a string of two or more closely driving vehicles traveling with a typically

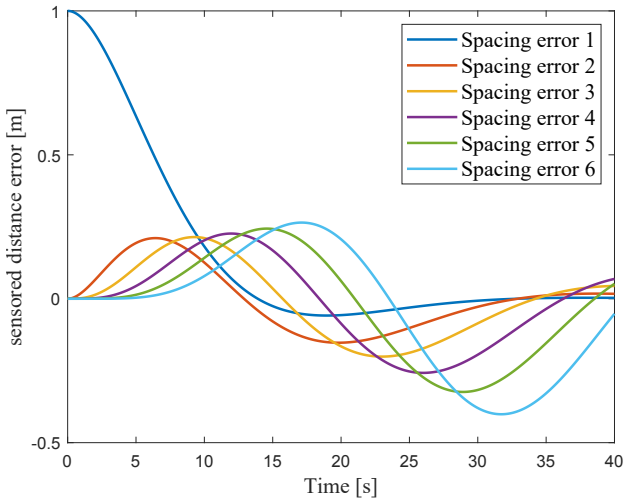

Fig. 2. Platooning system response to an initial disturbance.

very small desired distance between each vehicle, which can increase traffic throughput and improve aerodynamic efficiency. Additional benefits of platooning systems also include reducing aerodynamic drag and fuel consumption.

Despite these advantages, a major challenge in platooning control is string instability, i.e., a disturbance is amplified as it propagates along the string, as shown in Figure 2, which will cause emergent go-and-stop behavior. String stability has been the subject of extensive discussion and research [16]–[23]. Different definitions of string stability and analysis methods have been proposed over the years. Reference [24] thoroughly compared different string stability definitions and discussed the pros and cons of different analysis methods, which provide insight into selecting analysis methods for vehicle platoons in practice. To systematically study string stability, the platooning systems are classified based on the vehicle dynamics, how vehicles exchange information, the controller each vehicle is applied, and the desired inter-vehicle distance of the platoon system [25].

In this paper, we focus on a platooning system where each vehicle is modeled as a second-order system with a proportional-derivative (PD) controller, responding only to the immediately preceding vehicle as shown in Figure 1. In traditional models, integer-order derivatives are often used to describe dynamics [26]–[28], but they may not fully capture non-local interactions resulting from the control architecture in large-scale platoons. Therefore, we are interested in identifying the cases where the fractional order model can provide a better reduced-order model for a large-scale platooning system. By analyzing this simplified representation, we seek insights that can contribute to the design of more efficient control strategies to improve string stability.

The primary contributions of this paper are examining the fractional reduced-order modeling method and uncovering the relationship between model order and platooning control gains using an optimization-based approach. We analyze the modeling error of our proposed fractional-order model by comparing it with a reduced-order integer model—specifically, a second-order differential equation—while ensuring a comparable number of optimization decision variables for a fair comparison. The results indicate that circumstances, the fractional-order model outperforms the second-order model even with fewer optimization variables.

II. FRACTIONAL CALCULUS

This section briefly introduces fractional calculus. The starting point is Cauchy's formula for repeated integration, given by

$$\begin{aligned} D^{(-n)}f(t) &= \int_a^t \int_a^{\sigma_1} \cdots \int_a^{\sigma_{n-1}} f(\sigma_n) d\sigma_n \cdots d\sigma_1 \\ &= \frac{1}{(n-1)!}\int_a^t (t-z)^{n-1} f(z) dz. \end{aligned}$$

To generalize the integration to the fractional order, we can replace the factorial $(n-1)!$ with the gamma function $\Gamma(\alpha)$,

$$D^{(-\alpha)}f(t) = \frac{1}{\Gamma(\alpha)}\int_a^t (t-z)^{\alpha-1} f(z) dz.$$

In this way, the order of integration $n \in \mathbb{Z}$ is generalized to be $\alpha \in \mathbb{R}$. The gamma function $\Gamma(\cdot)$ is considered a generalization of factorial, since $n! = \Gamma(n+1)$. In other words, the factorial is equal to the Gamma function sampled at the integer values.

At this point, we introduce the Caputo definition of the fractional derivative. The key idea is to leverage the inverse relationship between integration and differentiation. For example, the operator $D^{1/2}$ can be interpreted as performing a half-order integration (fractional order) followed by a first-order differentiation (integer order). More generally,

$$\mathrm{D}^{\alpha}[f(t)] = \frac{1}{\Gamma(\lceil\alpha\rceil-\alpha)}\int_a^t (t-z)^{(\lceil\alpha\rceil-\alpha-1)} \frac{d^{\lceil\alpha\rceil} f}{dz^{\lceil\alpha\rceil}}(z)\mathrm{d}z,$$

where the ceiling function $\lceil\alpha\rceil$ gives the least integer greater than or equal to α. The Caputo derivative is adopted in this paper.

Essentially, fractional derivatives generalize integer-order derivatives by extending the derivative order from integers to real numbers, providing a more flexible mathematical framework. Note that the fractional order derivative is defined using integration, which will include all the history of f, allowing the fractional derivatives to capture memory effects and long-range dependencies in a system. These characteristics make fractional derivatives a promising approach for modeling the dynamics of large-scale platooning systems.

It is well known that the solution to the fractional-order system

$$\frac{d^{\alpha}x_f}{dt^{\alpha}} + ax_f(t) = 0, \quad \alpha \in (1,2)$$

$$x(0) = 0, \quad \dot{x}(0) = c,$$

is

$$x_f = ct^{\alpha-1}E_{\alpha,\alpha}(-at^{\alpha}), \tag{1}$$

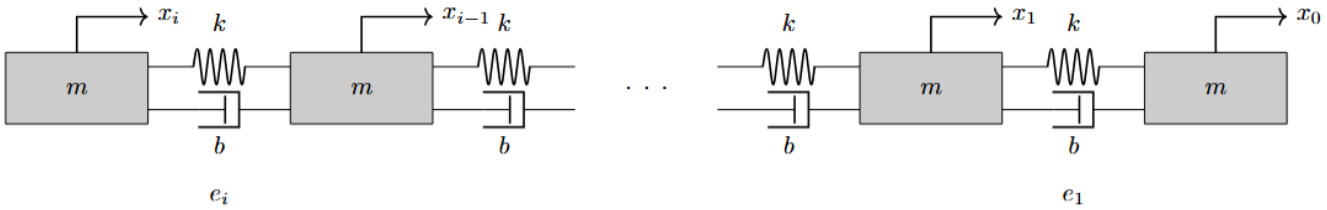

Fig. 3. Platoon network system.

where the Mittag-Leffler function is

$$\mathrm{E}_{\alpha,\beta}(t) = \sum_{k=0}^{\infty} \frac{t^k}{\Gamma(\alpha k + \beta)}, \quad \alpha, \beta > 0.$$

Compared with the exponential function written as a series,

$$e^t = \sum_{k=0}^{\infty} \frac{t^k}{\Gamma(k+1)},$$

it is apparent that the Mittag-Leffler function is the generalization of the exponential function, and when $\alpha = \beta = 1$, the Mittag-Leffler function is the exponential function. Subsequently, we will use Equation 1 as the solution to the fractional reduced model.

III. PROBLEM FORMULATION

In the analysis here, the platooning system can be viewed as a modified mass-spring-damper system. As shown in Figure 3, vehicles can be represented as mass, and the PD controller gains on the relative space and speed can be represented as spring and damping constants. However, unlike the classical mass-spring-damper system, each mass is connected to its adjacent masses through springs and dampers, creating a bidirectional interaction, where forces are transmitted in both directions. The predecessor-follower scheme we chose makes this bidirectional influence no longer present. Instead, each mass is only influenced by its predecessor, resulting in a unidirectional interaction, where control signals flow strictly backward along the string of vehicles.

In such a case, the equation of motion of the ith mass is

$$\ddot{x}_i(t) = u_i(t),$$

where u_i is the control input. The spacing error is

$$e_i = x_i - x_{i-1} - x_d,$$

where x_d is the desired spacing distance in the platooning system. For simplicity, we let $x_d = 0$ for the rest of this paper, and with the PD controller, the control input u_i is

$$u_i = k_p e_i + k_d \dot{e}_i,$$

where k_p and k_d are the PD control gains. The equation of motion of the ith spacing error is

$$\ddot{e}_i(t) = k_p(e_i - e_{i-1}) + k_d(\dot{e}_i - \dot{e}_{i-1}).$$

For the presented simulations, set $m = 1$, $i \in [1, 100]$, $k_p \in [20, 50]$ and $k_d \in [20, 50]$. The initial condition is $e_1(0) = 1$ and all other $e_i(0) = 0$. The other initial condition

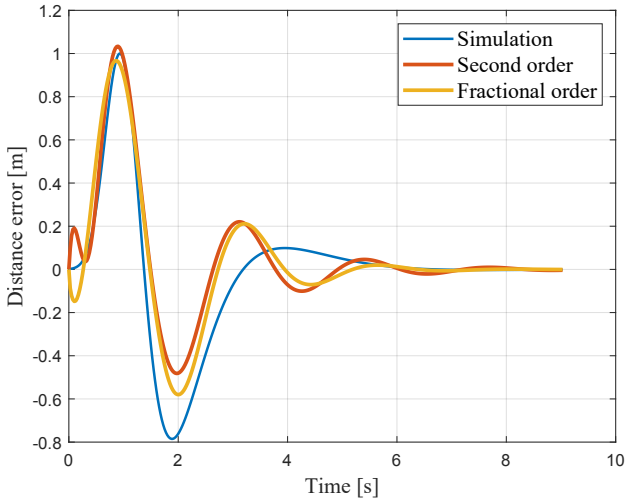

Fig. 4. Impulse response of the space error e_{100}.

is $\dot{e}_i(0) = 0$. We used MATLAB's `ode45` solver to simulate the differential equations for a system of 100 vehicles, and varying the parameters k_p and k_d between 20 and 50 produced several impulse-like responses. A typical response of e_{100} (the distance error between the last two vehicles) is shown in Figure 4 with $k_p = 32.5$ and $k_d = 35$, where the blue curve represents the simulation, the red curve represents the second-order model, and the orange curve represents the fractional-order model. The true system is of high order, arising from 100 coupled second-order equations, making exact fitting challenging. Nonetheless, the fractional-order model more closely approximates the simulation dynamics than the second-order model.

The next section introduces how we use an optimization-based method to search for the best parameters for the fractional reduced-order model, and we will propose a fair benchmark to the fractional reduced-order model for comparison.

IV. METHODS

As mentioned, we model the response of e_N as the solution to the fractional differential equation of the form in Equation 1. In our simulation setting, $N = 100$. We highlight here that the parameters $c, a \in \mathbb{C}$ and $\alpha \in \mathbb{R}$. We adopt the complex-valued form of the differential equation because we have found it has a superior ability to capture the system dynamics compared to the purely real formulation. Some discussion of the justification and limitations of modeling

in this way will be discussed in the Conclusions. As such, there are a total of 5 decision variables in the optimization, which are $[\mathrm{Re}(c), \mathrm{Im}(c), \mathrm{Re}(a), \mathrm{Im}(a), \alpha]$. The upper bound of these decision variables is $[15, 5, 5, 80, 2]$ and the lower bound is $[-5, -5, -5, -80, 1]$. The bounds were selected through trial and error to achieve the best optimization results observed. To find the best-matched solution, the sum of squared error (SSE) between the simulation result $e_N(t)$ and the real part of the fractional-order solution $x_f(t)$ is minimized

$$SSE_f = \sum_t \left(e_N(t) - \mathrm{Re}(x_f(t))\right)^2.$$

The reason why we need to take the real part of the fractional-order solution $x_f(t)$ is that in the optimization, we allow for complex coefficients.

To gauge the efficacy of using a fractional order approach, we also model the last space error e_N as the solution to a second-order differential equation x_s

$$\frac{d^2x_s}{dt^2} + 2\zeta\omega_n\frac{dx_s}{dt} + \omega_n^2 x_s = 0,$$

with initial conditions $x_s(0) = 0$, $\dot{x}_s(0) = b$ and complex coefficients. The parameters $\zeta, \omega_n, b \in \mathbb{C}$, i.e., there are a total of 6 decision variables, which are $[\mathrm{Re}(\zeta), \mathrm{Im}(\zeta), \mathrm{Re}(\omega_n), \mathrm{Im}(\omega_n), \mathrm{Re}(b), \mathrm{Im}(b)]$, with one more decision variable than the fractional order model, making it a challenging comparison to the fractional order model. The upper bound of these 6 decision variables is $[2, 1, 10, 6, 10, 150]$ and the lower bound is $[-2, -1, -10, -6, -10, -150]$, determined by trail and error. The closed-form solution is straightforward,

$$x_s = \frac{b}{\omega_d} e^{-\zeta\omega_n t} \sin\omega_d t,$$

where $\omega_d = \sqrt{1-\zeta^2}\ \omega_n$. Since all the parameters ζ, ω_n, and b are complex numbers, this solution is complex and, like above, the SSE between the simulation result $e_N(t)$ and the real part of the complex second-order solution $x_s(t)$ is minimized

$$SSE_s = \sum_t \left(e_N(t) - \mathrm{Re}(x_s(t))\right)^2.$$

Because the decision variable α in Equation 1 is the order of the fractional derivative as well as an exponent in the equation, we expect the optimization to be highly nonlinear with possibly numerous local minima. To ensure our results are not an artifact of a specific minimization method, two global optimizations are utilized. We use the hybrid particle swarm method and pattern search method — two fundamentally different approaches to reduce the likelihood that the outcomes are artifacts of a specific optimization algorithm. Both methods are implemented using standard MATLAB functions in the Global Optimization Toolbox.

For the hybrid particle swarm. First, a global search is performed using Particle Swarm Optimization (PSO). Upon completion of the PSO, we find that the best solution can be further refined using a local optimization method. We rely on a hybrid optimization scheme that pairs PSO with a gradient-based solver, fmincon. This local optimization solver uses the particle swarm's output as an initial guess, zooming in the region of interest with more precision. Within fmincon, we select the Sequential Quadratic Programming (SQP) algorithm for its robust convergence properties.

The pattern search method is also a gradient-free method that iteratively polls points in the neighborhood of the current best solutions. In this paper, the CompletePoll option is adopted, which enables the pattern search to search more points, thus potentially avoiding local minima.

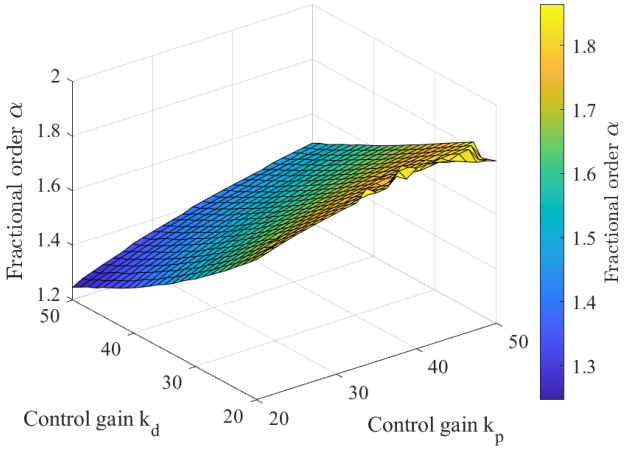

Fig. 5. Fractional order versus control gains.

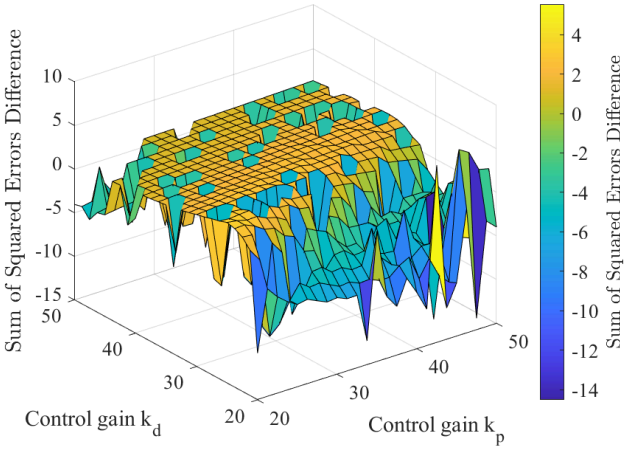

Fig. 6. The difference of the sum of squared error between the second-order system model and the fractional-order system model.

V. RESULTS

Figure 5 shows the main result in this paper and illustrates the relationship between the identified fractional order α and the control gain k_p and k_d. As shown in the figure, decreasing k_d leads to an increase in the fractional order α, while increasing k_p also leads to a higher α. Specifically, in the front corner of the figure, where both k_p and k_d are small, the searched order α is close to 1.7. On the left side

of the figure, where k_d is large and k_p is small, the searched order α is smallest and is close to 1.2. On the back of the figure, where k_p and k_d are both large, the searched order is close to 1.5. On the right side of the figure, where k_p is large and k_d is small, the searched order is the largest, and it is close to integer order 2. A few large variations observed in certain isolated regions suggest the optimization methods converged to a different, less optimal, local minima. Generally, simply re-running the optimization in these areas yields improved results and eliminates the large variations. The overall surface is generally regular and smooth, which indicates a systematic relationship between the control gains and the fractional order.

This result is intuitive when considering the mechanical system analogy, where the control gain k_p corresponds to the spring constant k, and k_d corresponds to the damping coefficient c. In a purely elastic system with only springs present, the system exhibits undamped harmonic oscillations, governed by a second-order differential equation. With the introduction of the dampers, the oscillation of the system is gradually suppressed. As damping increases, the system transitions from an under-damped system to a critically damped or over-damped system, where oscillations vanish. Although the system remains second-order in the integer-order framework, its behavior under high-damping conditions can resemble that of a first-order dynamic system. In the fractional-order framework, the effect is well captured by the order α, where variations in α between 1 and 2 reflect the degree of damping influence on the system's response.

Figure 6 illustrates the regions where the fractional-order model outperforms the second-order model and vice versa. The difference of the SSE is calculated as the SSE of the second-order model minus the SSE of the fractional-order model. Consequently, regions displayed in yellow indicate a positive difference, meaning that the fractional order model performs better. Conversely, regions shown in green indicate a negative difference, meaning that the second-order model performs better. This, in some sense, echoes the trend observed in Figure 5. Specifically, the fractional-order model achieves higher accuracy when the searched order is in an intermediate range, neither close to 1 nor 2. In contrast, the second-order model usually performs better as the searched order approaches 2. It is worth noting, in Figure 6, that multiple sharp concavities are evident, indicating regions where the objective function experiences rapid changes. Whether this behavior is associated with local minima or other system characteristics is still unclear and requires further research.

Figures 7 and 8 present the SSE of the fractional-order model and the second-order model, respectively. Both figures exhibit 'ridges' in about the same control gain regions, particularly where k_d is relatively small compared to k_p. The exact cause of this phenomenon requires further study; however, one possible explanation is that increased k_d effectively suppresses the system's higher-order dynamics, causing it to behave like a lower-order system. It is important to emphasize that the original system is a very high-order

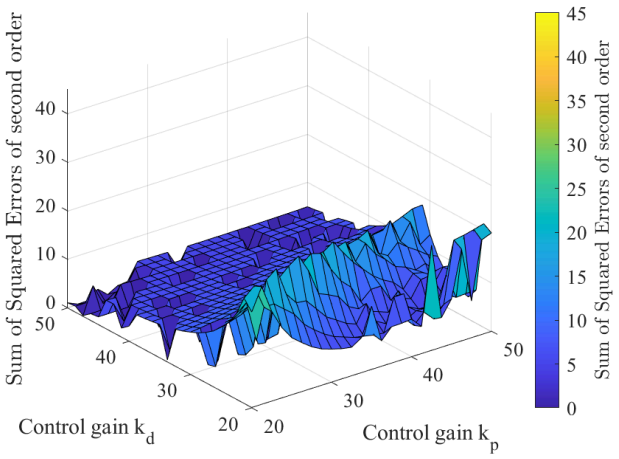

Fig. 7. Sum of squared error of the second-order system model.

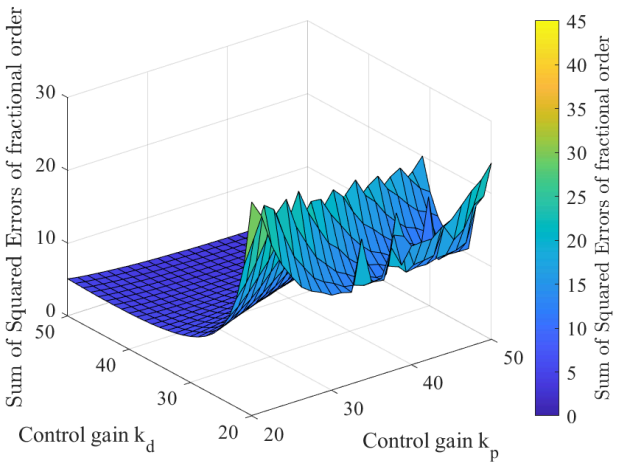

Fig. 8. Sum of squared error of the fractional order system model.

system consisting of 100 vehicles, each modeled as a second-order dynamic system. Consequently, the original system has approximately 200 orders. This may explain why both the fractional-order and second-order models struggle to accurately capture the system behavior in the regions where k_d is small, leading to poor performance.

VI. CONCLUSIONS AND FUTURE WORKS

This paper employs fractional-order dynamic modeling to analyze large platooning systems. Using an optimization-based method, it reveals the relationship between the control gains and the optimal model order. To investigate the performance of the fractional order model and ensure a fair comparison, a second-order integer model with a comparable number of decision variables is used as a benchmark. The results not only show when one model outperforms the other but also, from another perspective, justify the trend we observed regarding the relationship between the control gains and the optimal model order.

Although our experiments presented in this paper focus on a platooning system of a specific size, additional tests

with sizes 50 and 150 have shown that varying the size does not qualitatively affect the observed trend. While the optimization method allows us to identify a clear pattern in how the system order varies with different control gains, any deeper underlying mechanism driving this relationship remains unclear and requires further study.

Notably, the fractional-order and second-order models of the platooning system are represented as complex functions, which is uncommon. We chose complex-valued functions because, for the same model order, they capture system dynamics more accurately than their real-valued counterparts. The real part of the complex-valued model we adopt in the optimization has corresponding real-valued closed-form representations. However, these real-valued expressions are often more complicated, whereas the complex form offers a more concise and manageable representation. However, further research is needed to determine whether complex-valued functions are truly necessary and to clarify the role of each decision variable in the model.

Another limitation of this analysis is the presence of numerous concavities in the surface plot. As shown in Figure 6, positive values indicate that the fractional-order model outperforms the second-order model, while negative values suggest the opposite. However, the surface exhibits significant variations, with sharp concavities scattered across the control gain space. These concavities may result from local minima. This partially lies in the lack of insight into the physical meaning of the decision variables and the reliance on trial-and-error for selecting their optimization bounds.

From Figure 4, we can observe that even in the situation where the fractional model is better than the second-order model. The model error is still visible. Even though it is inevitable for us since we seek to obtain a significantly reduced order model. It gives us a direction where the fractional model has more potential modeling power than the integer order. However, one of the downsides of fractional calculus is that it requires more computational time. What is the good balance in capturing the system's important behavior, and computational time would be another future research direction.

REFERENCES

[1] M. D. Ortigueira, *Fractional calculus for scientists and engineers*, vol. 84. Springer Science & Business Media, 2011.

[2] K. Oldham and J. Spanier, *The fractional calculus theory and applications of differentiation and integration to arbitrary order*. Elsevier, 1974.

[3] A. Oustaloup, *La dérivation non entière*. No. BOOK, Hermes, 1995.

[4] A. Alessandretti *et al.*, "Finite-dimensional control of linear discrete-time fractional-order systems," *Automatica*, vol. 115, p. 108512, 2020.

[5] X. Ni and B. Goodwine, "Damage identification for the tree-like network through frequency-domain modeling," *IFAC-PapersOnLine*, vol. 53, no. 2, pp. 705–711, 2020.

[6] B. Goodwine, "Fractional-order dynamics in large scale control systems," in *31st Mediterranean Conference on Control and Automation (MED)*, IEEE, 2023.

[7] H. H. Sun, A. Abdelwahab, and B. Onaral, "Linear approximation of transfer function with a pole of fractional power," *IEEE Transactions on Automatic Control*, vol. 29, no. 5, pp. 441–444, 1984.

[8] M. Du, Z. Wang, and H. Hu, "Measuring memory with the order of fractional derivative," *Scientific Reports*, vol. 3, p. 3431, 2013.

[9] R. Meng *et al.*, "Fractional description of time-dependent mechanical property evolution in materials with strain softening behavior," *Applied Mathematical Modelling*, vol. 40, no. 1, pp. 398–406, 2016.

[10] K. Leyden, M. Sen, and B. Goodwine, "Large and infinite mass–spring–damper networks," *Journal of Dynamic Systems, Measurement, and Control*, vol. 141, no. 6, p. 061005, 2019.

[11] B. Goodwine and T. Chen, "Using a neural network trained only on integer order systems to identify fractional order dynamics in networked systems," in *2024 10th International Conference on Control, Decision and Information Technologies (CoDIT)*, pp. 2780–2785, IEEE, 2024.

[12] K. Bingi *et al.*, *Fractional-order systems and PID controllers*, vol. 264. Cham, Switzerland: Springer International Publishing, 2020.

[13] A. Oustaloup, X. Moreau, and M. Nouillant, "The crone suspension," *Control Engineering Practice*, vol. 4, no. 8, pp. 1101–1108, 1996.

[14] H. Li, J. Cheng, H.-B. Li, and S.-M. Zhong, "Stability analysis of a fractional-order linear system described by the caputo–fabrizio derivative," *Mathematics*, vol. 7, p. 200, 2019.

[15] P. Gong, Y. L. Wei, and Q.-L. Han, "Robust adaptive fault-tolerant consensus control for uncertain nonlinear fractional-order multi-agent systems with directed topologies," *Automatica*, vol. 117, p. 109011, 2020.

[16] J. Alleleijn, H. Nijmeijer, S. Öncü, and J. Ploeg, "Lateral string stability of vehicle platoons," *Vehicle System Dynamics*, vol. 52, no. 4, pp. 511–531, 2014.

[17] P. Barooah and J. P. Hespanha, "Error amplification and disturbance propagation in vehicle strings with decentralized linear control," in *Proceedings of the 44th IEEE Conference on Decision and Control (CDC-ECC)*, pp. 4964–4969, IEEE, 2005.

[18] B. Besselink and K. H. Johansson, "String stability and a delay-based spacing policy for vehicle platoons subject to disturbances," *IEEE Transactions on Automatic Control*, vol. 62, no. 11, pp. 5864–5879, 2017.

[19] P. Cook, "Conditions for string stability," *Systems & Control Letters*, vol. 54, no. 10, pp. 991–998, 2005.

[20] J. Eyre, D. Yanakiev, and I. Kanellakopoulos, "String stability properties of ahs longitudinal vehicle controllers," in *IFAC Proceedings Volumes*, vol. 30, pp. 71–76, IFAC, 1997.

[21] E. Shaw and J. K. Hedrick, "String stability analysis for heterogeneous vehicle strings," in *Proceedings of the American Control Conference (ACC)*, pp. 3118–3125, IEEE, 2007.

[22] D. Swaroop and J. K. Hedrick, "String stability of interconnected systems," *IEEE Transactions on Automatic Control*, vol. 41, no. 3, pp. 349–357, 1996.

[23] E. Abolfazli, B. Besselink, and T. Charalambous, "On time headway selection in platoons under the mpf topology in the presence of communication delays," *IEEE Transactions on Intelligent Transportation Systems*, vol. 23, no. 7, pp. 8881–8894, 2021.

[24] S. Feng, Y. Zhang, S. E. Li, Z. Cao, H. X. Liu, and L. Li, "String stability for vehicular platoon control: Definitions and analysis methods," *Annual Reviews in Control*, vol. 47, pp. 81–97, 2019.

[25] Y. Zheng, S. E. Li, K. Li, and L.-Y. Wang, "Stability margin improvement of vehicular platoon considering undirected topology and asymmetric control," *IEEE Transactions on Control Systems Technology*, vol. 24, no. 4, pp. 1253–1265, 2015.

[26] S. E. Li, Y. Zheng, K. Li, Y. Wu, J. K. Hedrick, F. Gao, and H. Zhang, "Dynamical modeling and distributed control of connected and automated vehicles: Challenges and opportunities," *IEEE Intelligent Transportation Systems Magazine*, vol. 9, no. 3, pp. 46–58, 2017.

[27] S. Stüdli, M. M. Seron, and R. H. Middleton, "From vehicular platoons to general networked systems: String stability and related concepts," *Annual Reviews in Control*, vol. 44, pp. 157–172, 2017.

[28] D. Martinec, I. Herman, Z. Hurák, and M. Šebek, "Wave-absorbing vehicular platoon controller," *European Journal of Control*, vol. 20, no. 5, pp. 237–248, 2014.